To appear in: Astronomy in the submillimeter and far infrared domains with the Herschel Space Observatory
Editors : will be set by the publisher
EAS Publications Series, Vol. ?, 2007

THE FORMATION OF LOW-MASS STARS WITH HERSCHEL

Patrick Hennebelle[1] and Frédérique Motte[2]

Abstract. We review the theories and the observations relevant for the formation of low-mass stars, particularly emphasizing the aspects that *Herschel* will contribute to develop.

1 Introduction

Star formation remains one of the most important and challenging problem of the modern astrophysics. Its complexity comes from the large range of relevant spatial and temporal scales in the problem and from the profusion of physical processes, often non linear, which are playing a role in the formation of stars.

We briefly review the theories and the observations which have been developed and carried out over the years, to explain the formation of low-mass stars. Since covering the whole topic in only a few pages is hopeless, we focus on the aspects which are more directly relevant in the context of the science that will be done with the *Herschel* space observatory. In particular, given the angular resolution of *Herschel*, we will address the scales of molecular clouds, clumps, and dense cores. The inner part of dense cores, associated with the disk, its fragmentation, and the launching of outflows are therefore excluded.

2 Formation of low-mass stars: theory

2.1 Overview

It is well established that stars form by gravitational collapse of molecular dense cores. These cores are themselves embedded in molecular clouds and often, though not always, inside filaments. However, the conditions through which the dense cores form, collapse and fragment remain a matter of debate.

[1] Ecole normale supérieure, 24 rue Lhomond, 75005 Paris, France
[2] Laboratoire AIM, CEA/DSM - CNRS - Université Paris Diderot, DA PNIA/SAp, CEA-Saclay, 91191 Gif-sur-Yvette Cedex, France

DOI: (will be inserted later)

In particular, a central and outstanding question, is the star formation efficiency through the Galaxy. As pointed out by Zuckermann and Evans (1974), if all the molecular gas observed in the Galaxy was collapsing in a freefall time, then the star formation rate, would be 10 to 100 times higher than the observed star formation rate $\simeq 3$ $M_\odot$ yr^{-1} observed in the Galaxy. A lot of efforts have been devoted to explain this low efficiency of star formation. Two main ideas have been explored so far. The first is that magnetic field provides an efficient support against gravity and delays the star formation (e.g. Shu et al. 1987). The second postulates that turbulent motions observed in molecular clouds, prevent the clouds to collapse in a freefall time (Mac Low & Klessen 2004).

In the following, we first present the basic theory of self-gravitating isothermal gas, including Jeans length, self-gravitating equilibrium and collapse. We then describe the effects induced by the magnetic field and the prediction of these models regarding dense cores. Finally, we expose the influence of the turbulence and its effects on the dense core formation.

2.2 Gravity and thermal support

Before going into the more complex situations of magnetized and turbulent clouds, it is important to establish the basic principles of self-gravitating isothermal gas dynamics.

2.2.1 Jeans length and freefall time

The Jeans length (Jeans 1905, Lequeux 2005) is easily derived by performing a linear analysis of the self-gravitating fluid equations. Let us consider a cloud of density ρ_0, radius R, and sound speed C_s (note that strictly speaking a self-gravitating isothermal cloud cannot have a uniform density because the pressure forces should compensate the gravitational forces). A linear analysis leads to the dispersion relation

$$\omega^2 = C_s^2 k^2 - 4\pi G\rho_0, \tag{2.1}$$

which reveals that when the wave number, k, is smaller than $\sqrt{4\pi G\rho_0}/C_s$, the waves cannot propagate and perturbations are amplified. From this we obtain the Jeans length, λ_J,

$$\lambda_J = \sqrt{\frac{\pi C_s^2}{G\rho_0}}, \tag{2.2}$$

where G is the gravitational constant. The Jeans length can be physically understood in the following way. Self-gravity tends to induce contraction in a time scale of the order of $1/\sqrt{G\rho_0}$. On the other hand, thermal pressure tends to reestablish uniform density in a sound wave crossing time, R/C_s. If $1/\sqrt{G\rho_0} < R/C_s$, then the waves cannot erase the pressure fluctuations induced by the gravitational contraction before the whole cloud collapses.

Equation 2.1 shows that, for an isothermal gas, the Jeans length decreases with density. Therefore, in a collapsing cloud the number of Jeans mass increases as the collapse proceeds. Based on this argument, Hoyle (1953) proposed the concept of recursive fragmentation by which a cloud is fragmenting more and more as it becomes denser. However, as shown by Eq. 2.1, the growth rate of the gravitational instability, decreases with k, meaning that the large scale perturbations evolve more rapidly than the smaller scale perturbations. This implies that some sort of equilibrium for the large scales is needed for the Hoyle's idea to work.

In general, it is not possible to analytically compute the time for a cloud to collapse. However, in the ideal case of a cold spherical cloud with uniform density, one can calculate it exactly (see e.g. Lequeux 2005). The result, known as the freefall time, is

$$\tau_{\rm ff} = \sqrt{\frac{3\pi}{32 G \rho_0}}. \tag{2.3}$$

2.2.2 Equilibrium configurations

Equilibrium configurations are obtained when pressure forces compensate gravitational forces. Such static solutions of the fluid equations are useful and convenient guides. They allow to test numerical codes, perform more rigorous stability analysis than the Jeans analysis and can sometimes be compared directly with the observations. The equations of equilibrium, namely the hydrostatic equation and the Poisson equation, are respectively:

$$-C_s^2 \partial_X \rho + \rho \partial_X \phi = 0, \tag{2.4}$$

$$\frac{1}{X^{D-1}} \partial_X (X^{D-1} \partial_X \phi) = -4\pi G \rho. \tag{2.5}$$

Combining these 2 equations leads to the so-called Lane-Emden equation:

$$\frac{1}{X^{D-1}} \partial_X \left(X^{D-1} \frac{\partial_X \rho}{\rho} \right) = -\frac{4\pi G}{C_s^2} \rho, \tag{2.6}$$

where D is the dimension and X the spatial coordinate.

In plane-parallel geometry ($D = 1$), X represents the usual Cartesian coordinate, z, whereas in cylindrical geometry ($D = 2$), X represents the cylindrical radius, r. In the first case, a self-gravitating layer solution has been inferred by Spitzer (1942) whereas in the second, a self-gravitating filament has been obtained by Ostriker (1964). These two solutions are fully analytical. They are characterized by a flat density profile near $X = 0$. The former presents an exponential decrease for large z whereas the latter decreases as r^{-4}.

In spherical geometry ($D = 3$) (X represents the spherical radius, r), the solutions of Eq. 2.6 are the so-called Bonnor-Ebert spheres (Bonnor 1956). In general, these solutions are not analytical and must be obtained by solving numerically Eq. 2.6. There is however a noticeable exception which is the singular isothermal

sphere whose density is given by $\rho_{\rm SIS} = C_s^2/2\pi G r^2$. The density profile of the Bonnor-Ebert sphere is flat in the inner part and tends toward the density of the singular isothermal sphere at large radii. Since it is physically required that the cloud has a finite radius, the solutions are obtained by truncating this profile at any arbitrary radius, assuming pressure equilibrium with the medium outside the cloud. This medium is supposed to be diffuse and warm. Therefore a whole family of equilibrium solutions is obtained. They can be characterized by the density contrast between the center and the edge. Stability analysis reveals that the solutions which have a density contrast smaller than about 14 are stable and unstable otherwise.

Stability analysis of the self-gravitating layer and filament have been performed in various studies (e.g. Larson 1985, Fiege & Pudritz 2000). Both are unstable to perturbations of wavelengths comparable to the Jeans length. In particular, this suggests that cores distributed periodically, could develop by gravitational instability within self-gravitating filaments.

2.2.3 Gravitational collapse

The gravitational collapse of a spherical cloud has been investigated in some details both analytically and numerically. Since even in spherical geometry, the cloud is described by 2 variables non linear equations, the analytical models have mainly focused on self-similar solutions (e.g. Larson 1969; Penston 1969; Shu 1977; Whitworth & Summers 1985) which allow to reduce the equations of the problem to simpler ordinary equations. These solutions have been useful to understand the physics of the collapse and sometimes used in various contexts to provide easily time-dependent density and velocity fields. Two main types of solutions have been inferred. Larson (1969) and Penston (1969) derive a solution which presents supersonic infall velocity at large radii ($\simeq 3.3 C_s$) whereas Shu (1977) obtains a solution in which the gas is initially at rest and undergoes inside-out collapse. A rarefaction wave which propagates outwards at the sound speed, is launched from the cloud center when the protostar forms. All self-similar solutions have constant accretion rate equal to few up to several times C_s^3/G. Note that in all solutions the density field is proportional to r^{-2} in the outer part and to $r^{-3/2}$ in the inner region which has been reached by the rarefaction wave. Finally, note that the density of the Larson-Penston solution is few times (4 to 7) larger than the density of the Shu's solution.

The collapse has also been investigated numerically. Larson (1969) starts with a uniform density cloud and calculates the gas contraction up to the formation of the protostar by using some simplified radiative transfer (see also Masunaga & Inutsuka 2000). He shows that a first accretion shock develops at the edge of the thermally supported core which forms when the dust becomes opaque to its own radiation, i.e. at a density of about 10^{-13} g cm^{-3}. This core is sometimes called the first Larson core. A second accretion shock forms at the edge of the protostar at much higher density ($\simeq 10^{-2}$ g cm^{-3}). Foster & Chevalier (1993) start with a slightly unstable Bonnor-Ebert sphere. Interestingly, they find that the collapse

occurs very slowly in the outer part where only subsonic infall velocities develop. In the inner part, however, supersonic motions appear. Indeed, they show that convergence towards the Larson-Penston solution is achieved deep inside the cloud. On the other hand, in the outer part of the envelope, the density profile turns out to stay close to $\rho_{\rm SIS}$. Triggered collapse has also been investigated by various authors (e.g. Hennebelle et al. 2003). Faster infall velocities are then obtained as well as densities few times denser than $\rho_{\rm SIS}$. A common feature shared by the numerical solutions is that the accretion rate varies significantly along time, unlike what is inferred from the self-similar solutions.

2.3 Influence of magnetic field

As recalled previously, magnetic field has early been proposed to provide an important mechanical support to the gas (see e.g. Shu et al. 1987) which could possibly explain the low star formation efficiency within the Milky Way. In this section, we expose the basic principles of the magnetically controlled theory of star formation.

2.3.1 Magnetic support and magnetic braking

The effect of the magnetic field is not easy to visualize because unlike the thermal pressure, it is highly non isotropic. In particular, the magnetic forces, $\mathbf{j}\times\mathbf{B}$, where $\mathbf{j}$ is the electric current, vanishes along the field lines. An easy way to estimate the magnetic support, is to compute the ratio of the magnetic over gravitational energies. For simplicity let us consider again a spherical and uniform cloud of mass M, volume V, radius R, threaded by an uniform magnetic field of strength B. The magnetic flux within the cloud, ψ is equal to $\psi=\pi R^2 B$. As long as the magnetic field remains well coupled to the gas (see next section), the magnetic flux threading the cloud will remain constant along time. The ratio of magnetic over gravitational energies for uniform density cloud threaded by a uniform magnetic field, is:

$$\frac{E_{\rm mag}}{E_{\rm grav}}=\frac{B^2V}{8\pi}\times\frac{2R}{5GM^2}\propto\frac{B^2R^4}{M^2}\propto\left(\frac{\psi}{M}\right)^2. \qquad (2.7)$$

Remarkably, the ratio of magnetic over gravitational energies is independent of the cloud radius. This implies that if the cloud contracts or expands, the relative importance of these two energies remains the same. This is unlike the thermal energy of an isothermal gas, which becomes smaller and smaller compared to the gravitational energy as the cloud collapses. It is clear from Eq. 2.7, that there is a critical value of the magnetic intensity for which the gravitational collapse is impeded even if the cloud was strongly compressed. Mouschovias & Spitzer (1976) have calculated accurately the critical value of the mass-to-flux ratio using the Virial theorem and numerical calculations of the cloud bidimensional equilibrium. A cloud which has a mass-to-flux ratio smaller than this critical value cannot collapse and is called

supercritical (subcritical). It is usual to define $\mu = (M/\psi)/(M/\psi)_{\rm crit}$. Large values of μ correspond to small magnetic fields and thus supercritical clouds.

Another important effect of the magnetic field is its ability to brake a rotating cloud. This is due to the generation of torsional Alfvén waves which propagate and transfer angular momentum from the cloud to the intercloud medium (Shu et al. 1987). To estimate the time scale over which this process is occurring, let us consider an intercloud medium of density $\rho_{\rm icm}$ and let us assume that the magnetic field is parallel to the rotation axis. The waves propagate at the Alfvén speed, $V_a = B/\sqrt{4\pi\rho_{\rm icm}}$ along a cylinder parallel to the magnetic field. Significant braking will arise when the waves have transmitted to the intercloud medium a substantial fraction of the cloud angular momentum. This is the case, when the waves have reached a distance from the cloud, l, such that $l \times \rho_{\rm icm} \simeq R \times \rho_0$. That is to say the waves have been able to transfer angular momentum to a mass of intercloud medium comparable to the mass of the cloud. This gives an estimate for the magnetic braking time, in case where the magnetic field and the rotation axis are aligned:

$$\tau_{\rm br} \simeq \frac{R}{V_a}\frac{\rho_0}{\rho_{\rm icm}}. \tag{2.8}$$

The braking time increases when $\rho_{\rm icm}$ decreases because if the intercloud medium has a low inertia, its angular momentum is small. Another important configuration is the case where the magnetic field and the rotation axis are perpendicular. Similar considerations show that the braking time is proportional in this case to $\sqrt{\rho_0/\rho_{\rm icm}}$. The difference with the preceding case is that the angular momentum is transmitted in the equatorial plane and not along the pole. Therefore the radius of the cylinder inside which the waves have propagated, grows with time.

Since the densities of the cloud and intercloud medium are usually very different, these relations show that the braking occurs more rapidly in the second case. Therefore, magnetic braking tends to align rotation axis and magnetic field.

2.3.2 Ambipolar diffusion

Until now, we have assumed that the magnetic field and the gas were perfectly coupled, implying field freezing. However at microscopic scales, the neutrals are not experiencing the Lorenz force which applies only on charged particles. Strictly speaking, this implies that at least two fluids should be considered, the neutrals and the ions (in different contexts more than one fluid of charged particles must be considered), to treat the problem properly. Since the two fluids are coupled to each other by the collisions, the neutrals are nevertheless influenced by the magnetic field if the gas is sufficiently ionized. Treating two fluids constitutes a significant complication that one is willing to avoid. On the other hand, since the ionization in molecular clouds is usually of the order of 10^{-7}, the density of the ions is much smaller than the density of the neutrals. It is thus possible to neglect the inertia of the ions and assume mechanical equilibrium between the Lorenz force and the

drag force. This leads to:

$$\frac{(\nabla \times \mathbf{B}) \times \mathbf{B}}{4\pi} = \gamma \rho \rho_i (\mathbf{V} - \mathbf{V}_i), \tag{2.9}$$

where ρ_i and $\mathbf{V_i}$ are the ions density and velocity respectively, $\gamma \simeq 3.5 \times 10^{13}$ cm^3 g^{-1} s^{-1} is the drag coefficient (Mouschovias & Paleologou 1981). From Eq. 2.9, the ions velocity can easily be expressed as a function of the neutral velocity and the Lorenz force. Considering now the induction equation, which entails the velocity of the ions, and using Eq. 2.9, we obtain

$$\partial_t \mathbf{B} + \nabla \times (\mathbf{B} \times \mathbf{V}) = \nabla \times \left(\frac{1}{4\pi\gamma\rho\rho_i} ((\nabla \times \mathbf{B}) \times \mathbf{B}) \times \mathbf{B} \right). \tag{2.10}$$

The left part of this equation is identical to the induction equation except that the velocity of the neutrals appears instead of the velocity of the ions. The right term is directly responsible for the slip between the neutrals and the magnetic field. Although it is of the second order, it is not rigorously speaking a diffusion term. From this equation, it can easily be inferred a typical timescale for the ambipolar diffusion.

$$\tau_{\rm ad} \simeq \frac{4\pi\gamma\rho\rho_i L^2}{B^2}, \tag{2.11}$$

where L is the typical spatial scale relevant for the problem. In the context of star formation, L could be the size of the cores, R. Ionization equilibrium allows to estimate that the ions density is about $\rho_i = C\sqrt{\rho}$, where $C = 3 \times 10^{-16}$ cm$^{-3/2}$ g$^{1/2}$.

If a dense core is initially subcritical (therefore magnetically supported), the diffusion of the field will progressively reduce the magnetic flux within the cloud. So after a few ambipolar diffusion times, the cloud is becoming supercritical and the magnetic field is not able to prevent the collapse any more. The important and interesting question at this stage is, how much is the collapse delayed by this process? In order to estimate this time, it is usual to assume that the cloud is in Virial equilibrium that is to say: $B^2/4\pi \simeq M\rho G/R$ (within a factor of a few) and to compute the ratio of $\tau_{\rm ad}$ and $\tau_{\rm ff}$, the freefall time (Shu et al. 1987). This leads to:

$$\frac{\tau_{\rm ad}}{\tau_{\rm ff}} \simeq 8. \tag{2.12}$$

Remarquably enough, $\tau_{\rm ad}/\tau_{\rm ff}$ is independent of R and M, the size and mass of the cloud (as long as the Virial assumption is verified). The important point is of course that $\tau_{\rm ad}$ is roughly 10 times higher than $\tau_{\rm ff}$. The implication is therefore that ambipolar diffusion could possibly reduce the star formation rate significantly making it closer to the observed value.

2.3.3 Prediction of ambipolar diffusion theory

In order to make quantitative predictions, numerical simulations of magnetized collapse controlled by ambipolar diffusion, have been performed (e.g. Basu & Mouschovias 1995). These simulations are generally one dimensional and assume a thin disk geometry. They explore a wide range of magnetic intensities, from nearly critical cores, $\mu \simeq 1$, to very subcritical cores, $\mu \ll 1$. They also investigate the effect of changing the ionization which results in a weaker coupling between the magnetic field and the gas. Velocity and density profiles potentially useful for comparison with observations, are therefore available in the literature. Here we simply draw some of the most important features.

When the dense core is very subcritical, with values of μ as low as 0.1, Basu & Mouschovias (1995) found that the infall velocity in the outer part of the envelope is only a small fraction of the sound speed with values as low as $0.2 \times C_s$ whereas in the inner part, it gradually increases and reaches values of about $0.5 - 0.8 \times C_s$. The collapse is significantly delayed and occurs in about 15 freefall times. For nearly critical cores, $\mu \simeq 1$, the infall velocity is roughly twice higher than in the previous case whereas the collapse occurs after about $\simeq$3 freefall times. Another interesting prediction, is the evolution of the central mass-to-flux ratio. The value of μ in the centre, smaller than 1 initially, grows with time as the cloud loses its flux and eventually becomes larger than 1. By the time, of protostar formation, typical values of μ are about $\simeq$2. Interestingly, this does not depend too much on the initial value of μ. An important prediction of the magnetically controlled models, is therefore that typically, values of μ around 2 should be measured. Values significantly higher than 2, would certainly indicate that the collapse is not magnetically controlled.

2.4 Role of turbulence

The theory of magnetically controlled star formation, has been challenged by a new theory based on supersonic turbulence (e.g. Mac Low & Klessen 2004) which has been developed during the last decade. The general idea of this theory is that turbulence prevents most of the gas to collapse in a freefall time and regulates the star formation. Slightly different aspects have nevertheless been emphasized by various authors.

2.4.1 Turbulent support and decay of turbulence

Unlike magnetic field, it is not straightforward to anticipate the influence of turbulence on the star formation rate. This is because, on one hand, the turbulent motions tend to spread out the gas, reducing its ability to collapse, but on the other hand, the turbulent motions may also increase the gas density locally when the flow is globally convergent. Moreover, the difficulty with theories involving turbulence is that it appears hopeless to search for exact analytical descriptions, even for highly idealized situations. Therefore most of our theoretical knowledge of the interstellar turbulence is provided by numerical simulations. It appears

nevertheless highly wishable to draw simple trends. To this purpose let us assume that the turbulence is sufficiently isotropic and is an additional support that can be described by a sound speed. Let $V_{\rm rms}$ be the root mean square of the velocity. The effective sound speed of the flow is $C_{\rm s,eff} \simeq \sqrt{C_s^2 + V_{\rm rms}^2/3}$. Since the turbulence observed in molecular clouds is highly supersonic, $V_{\rm rms}^2$ is larger than C_s^2 by typically a factor of 25 to 100. Therefore, $C_{\rm s,eff} \simeq V_{\rm rms}/\sqrt{3}$ and the turbulent Jeans mass, $M_J \propto V_{\rm rms}^3/\sqrt{\rho}$. On the other hand, turbulence creates density enhancements that can be estimated by the Rankine-Hugoniot jump conditions for an isothermal gas, $\rho/\rho_0 = (V/C_s)^2$, where ρ_0 is the mean cloud density. Combining these two relations, we get the turbulent Jeans mass $M_J \propto V_{\rm rms}$, which indicates that turbulence is globally supporting the cloud.

To go further than these very simple analytic estimates, it is necessary to perform numerical calculations. Before describing some results of these simulations, it is necessary to emphasize the fast decay of turbulence which constitutes a severe issue of the turbulent theory. Considering a turbulent piece of fluid of size L, a robust conclusion, seems to be that a significant fraction (say more than half) of the initial turbulent energy is dissipated in about one crossing time, $L/V_{\rm rms}$. This result, well established in the case of nearly incompressible fluids, has also been inferred for numerical simulations of supersonic turbulence with and without magnetic field (Mac Low & Klessen 2004). Therefore, if not driven (that is to say when no external forcing is applied continuously to the flow), the turbulence decays quickly and thus cannot delay very significantly the collapse of a self-gravitating cloud. In order to explain the low star formation rate in the Galaxy, the turbulence theory must invoke a driving source which continuously replenishes the turbulent energy. At the present time, this constitutes a major problem of this theory.

Various numerical simulations have been performed to study directly the influence of the turbulence on star formation. The complete descriptions of these studies cannot be achieved within the scope of this short summary and only some of the most important aspects are described below.

2.4.2 Hydrodynamical turbulence

As anticipated above, decaying turbulence cannot delay star formation significantly. Calculations done by Klessen et al. (2000) and Bate et al. (2003), indeed, show that within a few freefall times, most of the gas has been accreted. We note that, an interesting results has been obtained in this context. Bate et al. (2003) find that the mass distribution of the stars formed by gravitational collapse in their simulations closely follows the shape of the initial mass function of stars (IMF).

Driven turbulence can reduce the star formation rate if the driving is sufficient. With a large scale driving (that is to say $k = 1 - 2$ where k counts the number of driving wavelengths in the box), providing an effective Jeans mass of 0.6 in a box which contains a total mass equal to 1 (that is to say that the box contains more than one turbulent Jeans mass), Klessen et al. (2000) find that more than half of the mass is accreted within one freefall time. The problem is less severe if the driving is on smaller scales ($k = 3 - 4$ or $k = 7 - 8$) since in that case 3 to 6

(depending on the scales at which driving is applied) freefall times are needed to accrete half of the mass. If the driving is stronger, providing and effective Jeans mass of 3.2, these numbers are typically multiplied by a factor of 3 to 4. Star formation can be entirely suppressed if sufficiently strong driving is applied at scales smaller than the thermal Jeans length inside the box. Klessen et al. (2005) infer statistical properties of the sample of cores formed in their simulations. In particular, they find that roughly 40% of the cores have subsonic internal velocity dispersion, 40% transonic and 20% supersonic.

2.4.3 Turbulence in magnetized clouds without ambipolar diffusion

Driven turbulence in supercritical clouds has first been investigated by Padoan & Nordlund (1999). In the absence of gravity and assuming isothermal equation of state, they find that super Alfvénic clouds, that is to say clouds for which the Alfvén speed is smaller than $V_{\rm rms}$, match better the observed molecular clouds than the trans-Alfvénic clouds. Padoan & Nordlund (2002) also infer that dense cores formed in super-Alfvénic simulations, have a mass distribution which resemble the IMF.

Decaying and driven turbulence with self-gravity have been respectively investigated by Gammie et al. (2003) and Vázquez-Semadeni et al. (2005) for various field strengths. Various clumps and cores properties such as shape, correlation with magnetic field, mass spectrum or age, have been inferred from these simulations and often compare well with observations. In contrast to Padoan & Nordlund (1999), it has not been found in these works that the characteristics of super Alfvénic clouds match the observations better.

2.4.4 Turbulence in subcritical magnetized clouds with ambipolar diffusion

Turbulence in subcritical clouds in the presence of ambipolar diffusion, has been investigated by Basu & Ciolek (2004) and Li & Nakamura (2005). These simulations combine the magnetic support and the turbulent motions. Since the clouds are initially subcritical, ambipolar diffusion plays an important role since it allows to reduce locally the magnetic flux. Interestingly, it has been found that in this context turbulence tends to accelerate the star formation. This is because, turbulence creates stiff gradients, due to the formation of shocks, in which the ambipolar diffusion takes place quickly. Indeed, Eq. 2.11 shows that the ambipolar diffusion time decreases with the spatial scale, L.

A very interesting results is that these simulations are able to reproduce the low star formation efficiency observed in the Milky Way provided the initial value of μ is small enough (typically $\mu \simeq 1$) and the turbulence is sufficiently strong (typically $V_{\rm rms} \simeq 10 \times C_s$). As expected, all cores produced in these simulations, tend to be rather quiescent with typically subsonic motions.

3 Formation of low-mass stars: observations

3.1 A generally accepted scenario

Low- to intermediate-mass ($0.1 - 8\ M_{\odot}$) stars are forming within a molecular cloud which undergoes a series of contraction and fragmentation phases until the formation of a self-gravitating, starless cloud fragment called "pre-stellar dense core/condensation". Conceptually, the latter should be the initial core which will collapse to form a single or, at most, a binary star. Observationally, it may correspond to starless gravitationally-bound cloud structures which are dense ($10^4 - 10^6$ cm^{-3} volume-averaged densities), small-scale ($\sim$0.01–0.1 pc diameters), and cold ($\sim$10–20 K mass-averaged temperatures). At some point, a stellar embryo forms within the initial core which then enters the "protostellar phase". There, the protostar accretes material from its circumstellar infalling envelope and drives an outflow which maybe removes its angular momentum. As soon as the protostellar envelope dissipates, it reveals of "pre-main sequence/T Tauri star" surrounded by first a protoplanetary disk and then a debris disk.

The above scenario has been established thanks to an empirical evolutionary sequence derived from infrared surveys and (sub)millimeter maps of solar-type young stellar objects (YSOs) (see e.g. Fig. 1). First, depending on their infrared spectral index, low-luminosity YSOs have been divided into three classes: Class I $\rightarrow$ Class II $\rightarrow$ Class III, from evolved protostars to classical, and then weak T Tauri stars (Lada 1987). On the basis of (sub)millimeter dust continuum observations, the YSO classification scheme has then been extended toward younger sources with the addition of the stages of Class 0 protostars and pre-stellar cores (André et al. 1993; Ward-Thompson et al. 1994). In this classification, pre-stellar cores represent the initial core on the verge of collapse. Class 0 sources, distinguished by large submillimeter to bolometric luminosity ratios and self-embedded in massive circumstellar envelopes, are believed to be young protostars at the beginning of the main accretion phase. Class I sources are interpreted as more evolved protostars which have already accumulated the majority of their final stellar mass but are still accreting matter from a residual envelope. Class II and Class III YSOs correspond to pre-main sequence stars surrounded by a circumstellar disk, which is optically thick and optically thin, respectively. The empirical observational classification scheme of Class I to Class III sources was used to support the "standard" theory of low-mass star formation, which describes the ideal gravitational infall of a singular isothermal sphere originally at rest (e.g. Shu et al. 1987). In contrast, the characteristics of Class 0 and pre-stellar cores suggest that the initial dense core resembles more a Bonnor-Ebert sphere out of equilibrium (e.g. Foster & Chevalier 1993, Hennebelle et al. 2003). Sections 2.2.2–2.2.3 shortly present these two classes of models and Sect. 3.3 summarizes the existing constraints on the initial conditions of the collapse.

The earliest phases of low-mass star formation (i.e. pre-stellar cores and Class 0 protostars) are crucial to be studied because they are holding the key of the final mass of the star (see, e.g., the review by André et al. 2000). Mainly constituted

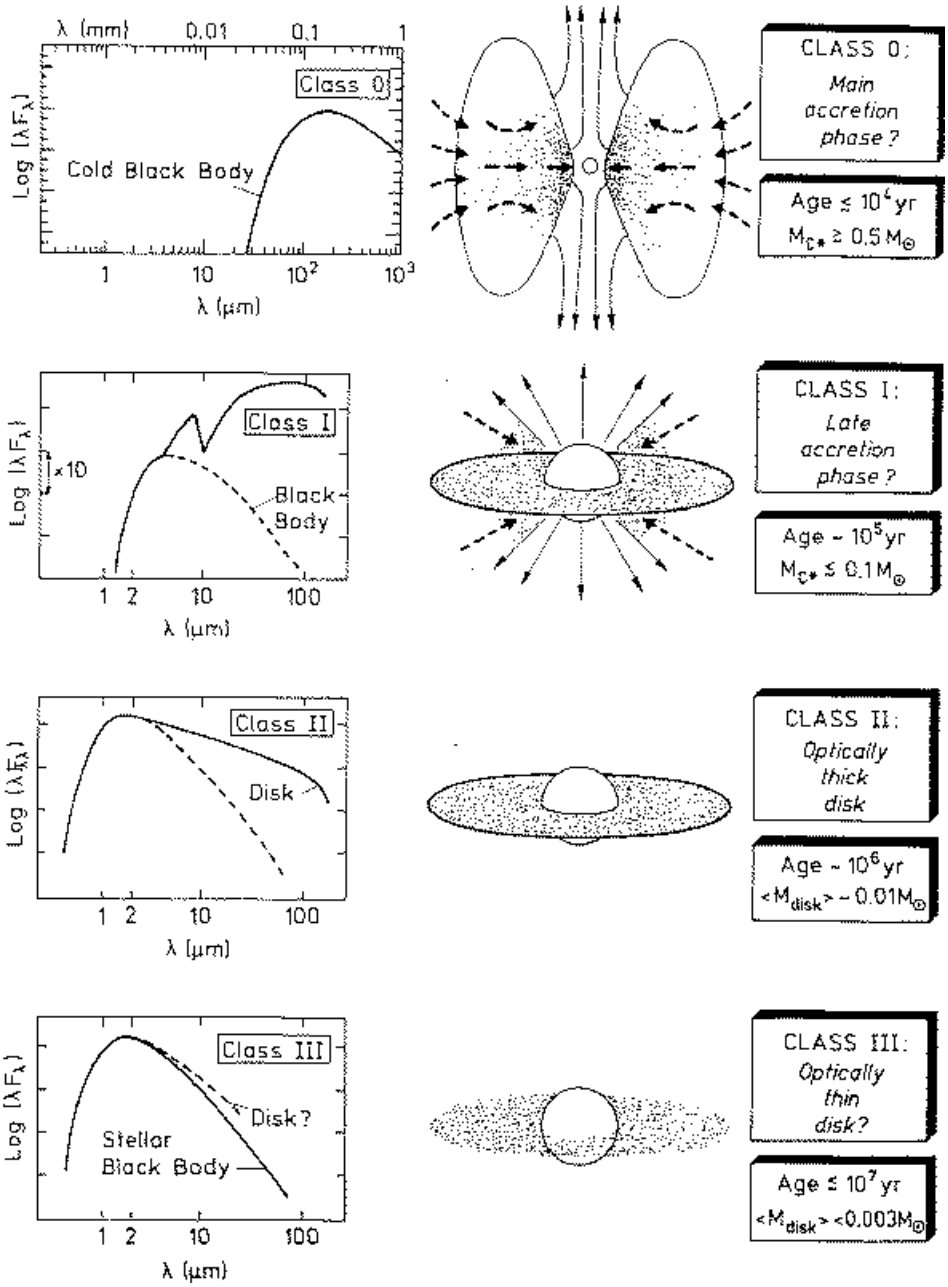

Fig. 1. Taken from André 1994: Evolutionary sequence of low-mass young stellar objects (with a stellar mass on the main sequence assumed to be 1 $M_{\odot}$) based on their spectral energy distributions (on the left) and their circumstellar masses (on the right).

of cold dense gas, these YSOs have spectral energy distributions peaking in the far-infrared to submillimeter range, around $100 - 200$ μm (see top left corner of Fig. 1). *Herschel* is uniquely suited to study these objects, especially because of its broad wavelength coverage of cold SEDs (see Fig. 3 of the chapter on high-mass star formation) and its unmatched resolution at far-infrared wavelengths. According to their typical sizes and masses, *Herschel* will be able to probe the pre-stellar cores and Class 0 protostars with enough resolution and sensitivity in star-forming regions located at up to 500 pc from our Sun. The unprecedented SPIRE-PACS wavelength coverage will give robust measurements of their spectral energy distributions, which, as shown in Fig. 1, is important for determining their evolutionary status.

3.2 The origin of the IMF: a fundamental open question

The question of the origin and possible universality of the initial mass function (IMF, see Salpeter 1955) is crucial for both star formation and galactic evolution but remains a matter of debate. Indeed, numerous molecular line studies of cloud structure have attempted, without success, to relate the mass spectrum of observed clumps to the stellar IMF (see, e.g., the review by Williams et al. 2000). There has recently been a growing body of evidence that the IMF of nearby star clusters is at least partly determined by pre-collapse cloud fragmentation. Indeed, ground-based (sub)millimeter continuum surveys of ρ Ophiuchi, Serpens, and Orion B revealed pre-stellar condensations whose mass distributions resemble the stellar IMF (Motte et al. 1998; Testi & Sargent 1998; Johnstone et al. 2000; Motte et al. 2001; Stanke et al. 2006; see e.g. Fig. 2). Therefore and at least in the low- to intermediate-mass range ($0.1 - 5$ $M_\odot$) probed here, these pre-stellar condensations could be the direct progenitors of protostars, i.e., the structures (initial cores) within which the individual protostellar collapse is initiated. A plausible scenario, supported by some numerical simulations of cluster formation (Klessen et al. 2000; Padoan et al. 2002), could be the following: First, cloud turbulence generates a field of density fluctuations, a fraction of them corresponding to self-gravitating fragments; second, these fragments (or "kernels") decouple from their turbulent environment and collapse to protostars after little interaction with their surroundings (e.g. Myers et al. 1998; André et al. 2007).

Present ground-based studies are limited by small-number statistics (in general less than 100 objects) and low sensitivity (usually objects have masses > 0.1 $M_\odot$). Deeper, more extensive, far-infrared to (sub)millimeter surveys should be done to search for the pre-stellar condensations more massive than 10 $M_\odot$ and less massive than 0.1 $M_\odot$. Surveys in a variety of star-forming regions (from our solar neighborhood to the Galactic center) are also clearly required to investigate possible environmental effects.

In that context, the "Gould Belt" (Probing the origin of the stellar IMF) Key Programme of *Herschel* aims at checking if the IMF is indeed determined by cloud fragmentation at the pre-stellar stage of star formation. Coordinated by André & Saraceno, this Guaranteed Time Key Programme is jointly proposed by the SPIRE

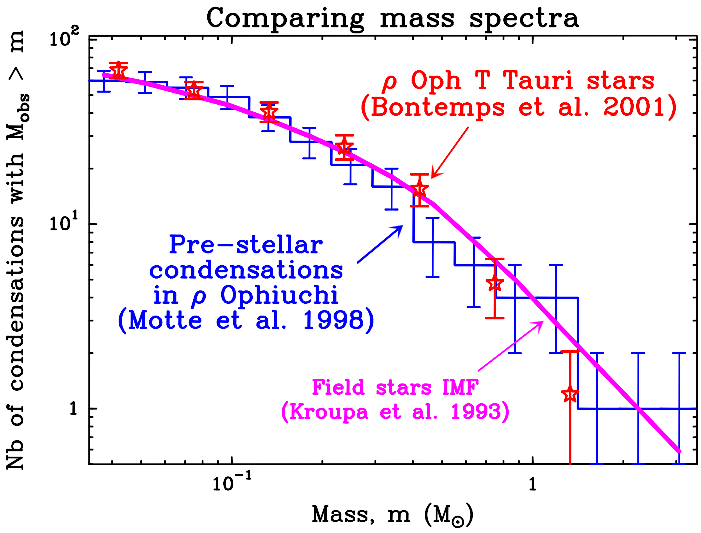

Fig. 2. Adapted from Motte et al. (1998) and Bontemps et al. (2001): Cumulative mass distribution of the pre-stellar condensations in the ρ Oph protocluster (blue histogram, complete down to $\sim$0.1 $M_\odot$) compared with the IMF of field stars (pink curve, Kroupa et al. 1993) and that of ρ Oph T Tauri stars (red star-like markers).

and PACS consortia, and the Herschel Science Centre (André & Saraceno 2005; see also http://starformation-herschel.iap.fr/gouldbelt/). The "Gould Belt" project will carry out unbiased photometric surveys, with both SPIRE and PACS, of the nearby ($d_{\rm Sun} = 100 - 500$ kpc) star-forming clouds composing the Gould Belt. It will therefore provide, for the first time, the mass and luminosity functions for complete samples of thousands of pre-stellar condensations and Class 0s down to the proto-brown dwarf regime ($0.01 - 0.08$ $M_\odot$) and up to intermediate-mass objects (up to 8 $M_\odot$). Such a study is expected to revolutionize our knowedge of the origin of the stellar IMF.

3.3 Initial conditions of the protostellar collapse

In order to distinguish between collapse models (see e.g. Sect. 2), observations of both the density and the velocity profiles of pre-stellar cores/condensations and protostellar envelopes are required. The density structure of well-recognized objects has been extensively investigated in submillimeter continuum emission (e.g. Ward-Thompson et al. 1994; Shirley et al. 2000; Motte & André 2001) and mid-infrared absorption (e.g. Bacmann et al. 2000; Alves et al. 2001). While protostellar envelopes generally follow a $\rho(r) \propto r^{-2}$ to $\propto r^{-1.5}$ density profile, pre-stellar cores ressemble more a Bonnor-Ebert sphere with a flattening at small radii and a sharp edge at some outer radius. In cluster-forming regions, the protostellar envelopes of Class 0 sources are generally denser than what is predicted for the

collapse of a thermally-supported initial core. It suggests either the existence of an additional support (turbulence and/or magnetic field) or initial conditions far from a quasi-static equilibrium. The results obtained on the density structure of the earliest phases of low-mass star formation seem to support the standard theory of the protostellar collapse in isolated regions and more dynamical scenarios in proto-clusters (see e.g. Motte & André 2001).

However, the above interpretations are very uncertain due to the fact that dust properties (temperature and emissivity) are unknown and generally assumed to be constant through pre-stellar dense cores/condensations and protostellar envelopes. *Herschel* will give more secure constraints on the initial conditions of the protostellar collapse by making simultaneous and direct measurements of both the density and temperature structures (e.g. André et al. 2004). The Garanteed Time Key Programmes of André & Saraceno ("Gould Belt") and Henning et al. (see Sect. 3.5 of the chapter on high-mass star formation) will make such analysis. Moreover, the large spatial dynamic range of the "Gould Belt" project will probe the link between diffuse interstellar medium and compact self-gravitating condensations, thereby setting strong constraints on possible core formation mechanism(s).

4 Conclusion

With the advent of the *Herschel* satellite and soon after the ALMA interferometer we are entering a very promissing era for the studies of the earliest phases of star formation. Large-scale imaging surveys complemented by high-resolution studies will surely solve many of the fundamental questions we currently ask ourselves, such as the origin of the stellar IMF and the initial conditions of the protostellar collapse.

References

Alves, J. F., Lada, C. J., Lada, E. A. 2001, Nature, 409, 159

André, Ph. 1994, in The cold universe, Montmerle, Lada, Mirabel, & Trân Thanh Vân (eds.), Éditions Frontières (Gif/Yvette), p. 179

André, Ph., Saraceno, P. 2005, in The dusty and molecular universe: a prelude to Herschel and ALMA, A. Wilson (ed), ESA SP-577 (Netherlands), p. 179

André, Ph., Ward-Thompson, D., Barsony, M. 1993, ApJ, 406, 122

André, Ph., Ward-Thompson, D., Barsony, M. 2000, in Protostars & Planets IV, ed. V. Mannings, A. Boss, & S. Russell (Tucson: Univ. Arizona Press), 59

André, P., Bouwman, J., Belloche, A., Hennebelle, P., 2004, Ap&SS, 229, 335

André, Ph., Belloche, A., Motte, F., Peretto, N. 2007, A&A, 472, 519

Bacmann, A., André, P., Puget, J.-L., et al. 2000, A&A, 361, 555

Basu, S., Ciolek, G. 2004, ApJ, 607, L39

Basu, S., Mouschovias, T. 1995, ApJ, 452, 386

Bate, M., Bonnell, I., Bromm, V. 2003, MNRAS, 339, 577

Bonnor, W. 1956, MNRAS, 116, 351

Bontemps, S., André, Ph., Kaas, et al. 2001, A&A, 372, 173
Fiege, J., Pudritz, R. 2000, MNRAS, 311, 105
Foster, J., Chevalier, R. 1993, ApJ, 416, 303
Gammie, C., Lin, Y.-T., Stone, J., Ostriker, E. 2003, ApJ, 592, 203
Hennebelle, P., Whitworth, A., Gladwin, P., André, Ph. 2003, MNRAS, 340, 870
Hoyle, F. 1953, ApJ, 118, 513
Jeans, J. 1905, ApJ, 22, 93
Johnstone, D., Wilson, C. D., Moriarty-Schieven, G., Joncas, G., Smith G. 2000, ApJ, 545, 3274
Klessen, R., Heitsch, F., Mac Low, M.-M. 2000, ApJ, 535, 887
Klessen, R., Ballesteros-Paredes, J., Vázquez-Semadeni, E., Durán-Rojas, C. 2005, ApJ, 620, 786
Kroupa, P., Tout, C. A., Gilmore, G. 1993, MNRAS, 262, 545
Lada, C.J. 1987, in Star forming regions, IAU Symp. 115, M. Peimbert & J. Jugaku (eds), p. 1
Larson, R. 1969, MNRAS, 145, 405
Larson, R. 1985, MNRAS, 214, 379
Lequeux, J. 2005, in The interstellar medium, J. Lequeux (ed), EDP Sciences (Berlin: Springer)
Li, Z.-Y., Nakamura, F. 2005, ApJ, 631, 411
Mac Low, M.-M., Klessen, R. 2004, Reviews of Modern Physics, 76, 125
Masunaga, H., Inutsuka, S.-i. 2000, ApJ, 531, 350
Motte, F., André, Ph. 2001, A&A, 365, 440
Motte, F., André, Ph., Neri, R. 1998, A&A, 336, 150
Motte, F., André, Ph., Ward-Thompson, D., Bontemps, S. 2001, A&A, 372, L41
Mouschovias, T., Spitzer, L. 1976, ApJ, 210, 326
Mouschovias, T., Paleologou, E. 1981, ApJ, 246, 48
Myers, P. C. 1998, ApJ, 469, L109
Ostriker, J. 1964 , ApJ, 140, 1056
Padoan, P., Nordlund, A. 1999, ApJ, 525, 318
Padoan, P., Nordlund, A. 2002, ApJ, 576, 870
Penston, M. 1969, MNRAS, 144, 425
Salpeter, E. E. 1955, ApJ, 121, 161
Shirley, Y., Evans II, N. J., Rawlings, J. M. C., Gregersen, E. M. 2000, ApJS, 131, 249
Shu, F. H. 1977, ApJ, 214, 488
Shu, F. H., Adams, F. C., Lizano, S. 1987, ARA&A 25, 23
Spitzer, L. 1942, ApJ, 95, 329
Stanke, T, Smith, M. D., Gredel, R., Khanzadyan, T. 2006, A&A, 447, 609
Testi, L., Sargent, A. I. 1998, ApJ, 508, L91
Vázquez-Semadeni, E., Kim, J., Shadmehri, M., Ballesteros-Paredes, J. 2005, ApJ, 618, 344
Ward-Thompson, D., Scott, P.F., Hills, R.E., André, Ph. 1994, MNRAS, 268, 276
Whitworth, A., Summers, D., 1985, MNRAS, 214, 1

Williams,, S. J., Blitz, L., McKee, C. F. 2000, in Protostars & Planets IV, ed. V. Mannings, A. Boss, & S. Russell (Tucson: Univ. Arizona Press), 97

Zuckerman, B., Evans, N. 1974, ApJ, 192, L149.